DESIGN AND CONTROL OF FORMATIONS
NEAR THE LIBRATION POINTS OF THE SUN-EARTH/MOON EPHEMERIS SYSTEM[*]

K. C. Howell and B. G. Marchand
Purdue University

ABSTRACT

The concept of formation flight of multiple spacecraft near the libration points of the Sun-Earth/Moon (SEM) system, offers as many possibilities for space exploration as technical challenges. The initial focus of this research effort was the dynamics and control of formation flight in the circular restricted three-body problem (CR3BP). Presently, these results are transitioned into the more complete *n*-body ephemeris model to incorporate other gravitational perturbations as well as solar radiation pressure (SRP). The continuous control techniques previously applied in the CR3BP are successfully implemented in the SRP perturbed *n*-body ephemeris model. The current effort focuses mostly on the continuous control of spherical formations but also presents a summary of some naturally existing formations.

INTRODUCTION

Much of the available research on formation flight focuses on Earth orbiting configurations, where the influence of other gravitational perturbations can be safely ignored. However, renewed interest in formations that evolve near the vicinity of the Sun-Earth libration points has inspired new studies regarding formation keeping in the three-body problem [1-14]. Some of these investigations focus on the simplified circular restricted three-body problem (CR3BP) [1-5]. Howell and Marchand [1] consider linear optimal control, as applied to nonlinear time varying systems, as well as nonlinear control techniques, including input and output feedback linearization. These control strategies are applied to a two spacecraft formation where the chief spacecraft evolves along a three-dimensional periodic halo orbit near the L_2 libration point. A detailed study of the nominal formation keeping costs over a 6-month period is presented for two types of configurations; for a constant relative separation distance, the chief-deputy line is assumed to remain (a) fixed relative to the rotating frame, or (b) fixed relative to the inertial frame.

Formations modeled in the CR3BP do represent a good starting point for a preliminary analysis. However, ultimately, any definitive formation keeping studies must be performed in the *n*-body ephemeris model, where the time invariance properties of the CR3BP are lost and, consequently, precisely periodic orbits do not exist near the libration points. For formations determined in the ephemeris model, previous studies are focused on linear optimal control [6-7] as well as discrete targeter methods [8-12]. More recent studies [15] also consider feedback linearization methods, nonlinear optimal control, and discrete control methods that exploit the natural flow near the libration points. In particular, the implementation of a Floquet controller, modified from that usually implemented for station keeping [13-14], leads to the identification of naturally existing formations and further allows for direct deployment into these configurations. The present study is a continuation of previous work [1, 15] on continuous and discrete control techniques for formations that evolve near the libration points in the Sun-Earth/Moon system, as determined in the ephemeris model.

DYNAMICAL MODEL

Background

In this investigation, the standard form of the relative equations of motion for the *n*-body problem, as formulated in the inertial frame $\left(\hat{X} - \hat{Y} - \hat{Z} \right)$, is employed. The effects of solar radiation pressure (SRP) are also incorporated. Hence, the dynamical evolution of each vehicle in the formation is governed by

$$^{I}\ddot{\overline{r}}^{P_2 P_s} = -\frac{\mu_q}{\left(r^{P_2 P_s} \right)^3} + \sum_{j=1, j \neq 2, s}^{N} \mu_j \left(\frac{\overline{r}^{P_s P_j}}{\left(r^{P_s P_j} \right)^3} - \frac{\overline{r}^{P_2 P_j}}{\left(r^{P_2 P_j} \right)^3} \right) = \overline{f}_{grav}^{(P_s)} + \overline{f}_{srp}^{(P_s)}. \tag{1.1}$$

For notational purposes, let P_2 denote the central body of integration, in this case the Earth. Then, P_s represents the spacecraft, and the sum over j symbolizes the presence of other gravitational perturbations. The SRP force vector, as discussed by McInnes [16], can be modeled as

$$\overline{f}_{srp}^{(P_s)} = \frac{k S_0 A}{m_s c} \left(\frac{D_0^{\ 2}}{d^2} \right) \cos^2 \beta \; \hat{n}, \tag{1.2}$$

where k denotes the absorptivity of the spacecraft surface ($k = 2$ for a perfectly reflective surface), S_0 is the energy flux measured at the Earth's distance from the Sun [W/m²], D_0 is the mean Sun-Earth distance [km], A represents the constant spacecraft effective cross sectional area [km²], c is the speed of light [km/sec], m_s is the spacecraft mass [kg], β is the angle of incidence of the incoming photons, $\hat{n}$ denotes the unit surface normal, and d [km] represents the Sun-spacecraft distance. The sample spacecraft implemented in this study is modeled after the Terrestrial Planet Finder (TPF) combiner spacecraft, assuming a 25-meter diameter and a spacecraft mass of 700 kg. The SRP force parameters are summarized in Table 1.

Table 1 – TPF Combiner S/C Parameters

k	1.4	c	299792.458 km/sec	A	4.9087×10^{-4} km²
S_0	1.358×10^3 W/m²	D_0	1.49597870×10^8 km	m_s	700 kg

Relative Motion In The Presence Of SRP

The equations of motion for both the chief and deputy spacecraft may be expressed in the following form,

$$^{I}\ddot{\overline{r}}_{I}^{P_2 C} = \overline{f}_{grav}^{(C)} + \overline{f}_{srp}^{(C)} + \overline{u}_C \left(t \right) = \overline{f}^{(C)} + \overline{u}_C \left(t \right), \tag{1.3}$$

$$^{I}\ddot{\overline{r}}_{I}^{P_2 D_i} = \overline{f}_{grav}^{(D_i)} + \overline{f}_{srp}^{(D_i)} + \overline{u}_{D_i} \left(t \right) = \overline{f}^{(D_i)} + \overline{u}_{D_i} \left(t \right), \tag{1.4}$$

where $\overline{u}_C \left(t \right)$ and $\overline{u}_{D_i} \left(t \right)$ denote the control accelerations required to maintain the desired nominal configuration, and $\overline{f}^{(C)}$ and $\overline{f}^{(D_i)}$ represent the net force acting on the chief spacecraft and the ith deputy vehicle, respectively. The numerical integration for all vehicles in the formation is performed in terms of inertial coordinates such that, for instance, $\overline{r}^{P_2 D_i} = x_i \hat{X} + y_i \hat{Y} + z_i \hat{Z}$. Hence, the vehicle velocities and accelerations are associated with the inertial frame (*I*) defined by the unit vectors $\hat{X}$, $\hat{Y}$, and $\hat{Z}$.

The chief spacecraft, or center of the formation, is assumed to evolve along a quasi-periodic Lissajous trajectory. Since this is a naturally existing solution in this regime, the baseline control acceleration $\overline{u}_C \left(t \right)$ is zero. The relative equations of motion for the ith deputy, then, are easily determined by subtracting Equation (1.3) from (1.4),

$$^{I}\ddot{\overline{r}}_{I}^{CD_i} = \left(\overline{f}_{grav}^{(D_i)} - \overline{f}_{grav}^{(C)} \right) + \left(\overline{f}_{srp}^{(D_i)} - \overline{f}_{srp}^{(C)} \right) + \overline{u}_{D_i} \left(t \right) = \Delta \overline{f}^{(D_i)} + \overline{u}_{D_i} \left(t \right). \tag{1.5}$$

The vector $\bar{r}^{CD_i}$ denotes the position of the ith deputy relative to the chief spacecraft while $\Delta\bar{f}^{(D_i)}$ represents the relative net force vector. Let $\bar{\rho}$ represent the desired nominal path of the deputy spacecraft, then, $\dot{\bar{\rho}}$ designates the nominal velocity vector, and $\bar{u}_{D_i}{}^{\circ}(t)$ denotes the associated nominal control effort such that,

$$\ddot{\bar{\rho}} = \Delta\bar{f}^{D_i{}^{\circ}} + \bar{u}_{D_i}{}^{\circ}(t).\tag{1.6}$$

The superscript "$\circ$" denotes evaluation on the nominal solution $\left(\bar{\rho},\dot{\bar{\rho}}\right)$. The error dynamics, defined by

$$^I\ddot{\bar{e}} = {}^I\ddot{\bar{r}}_I^{CD_i} - \ddot{\bar{\rho}} = \left\{\Delta\bar{f}^{D_i} - \Delta\bar{f}^{D_i{}^{\circ}}\right\} + \left\{\bar{u}_{D_i} - \bar{u}_{D_i}{}^{\circ}\right\} = \delta\Delta\bar{f}^{D_i} + \delta\bar{u}_{D_i}(t),\tag{1.7}$$

are easily determined by subtracting the nominal motion in Equation (1.6) from (1.5).

CONTINUOUS CONTROL IN THE EPHEMERIS MODEL

Previous studies by Howell and Marchand [1] demonstrate the efficiency and cost effectiveness of both input feedback linearization (IFL) and output feedback linearization (OFL) methods for continuous formation control in the CR3BP. The IFL controller is designed to force the error dynamics of each state variable to follow a critically damped response. The OFL controller, on the other hand, is applied only to force the radial separation between the spacecraft to track some specific value. Hence, no relative orientation requirements are imposed on the formation. The initial investigation [1] also demonstrates that a linear quadratic regulator (LQR), derived from optimal control theory, yields essentially an identical error response and control acceleration history as the input feedback linearization approach in this regime. However, the IFL controller is computationally much less intensive and, by comparison, conceptually simpler. This particular characteristic makes the IFL controller more suitable for implementation in the ephemeris model than LQR.

Input Feedback Linearization (IFL)

For the error dynamics outlined in Equation (1.7), the nominal solution corresponds to the zero vector, i.e., $\bar{e}(t) = \bar{0}$. Consistent with the previous definition of the IFL controller [1], suppose that a critically damped error response, characterized by a natural frequency ω_n, is desired. Then, the differential control input, $\delta\bar{u}_{D_i}(t)$, measured relative to the nominal control acceleration $\bar{u}_{D_i}{}^{\circ}(t)$, is determined as

$$\delta\bar{u}_{D_i}(t) = -\delta\Delta\bar{f} - 2\omega_n{}^I\dot{\bar{e}} - \omega_n{}^2\bar{e}.\tag{1.8}$$

The total control effort is then the sum of the nominal control input, $\bar{u}_{D_i}{}^{\circ}(t)$, and the differential control acceleration, $\delta\bar{u}_{D_i}(t)$.

To illustrate the effectiveness of the IFL controller, define a two spacecraft 50-m formation that is constrained to remain aligned with the inertial y-axis ($\hat{Y}$) at all times. The nominal relative motion is described by $\bar{\rho}(t) = (50\text{ m})\hat{Y}$ and $\dot{\bar{\rho}}(t) = \bar{0}$ m/sec. The chief spacecraft is assumed to evolve along a reference "halo" orbit near L_2 characterized by a 200,000 km maximum out-of-plane excursion. For an arbitrary injection error, relative to $\bar{\rho}$ and $\dot{\bar{\rho}}$, of the form $\delta\bar{r} = \left(7\hat{X} - 5\hat{Y} + 3\hat{Z}\right)$ km in position and $\delta{}^I\dot{\bar{r}} = \left(\hat{X} - \hat{Y} + \hat{Z}\right)$ m/sec in velocity, the total formation keeping cost, over a period of 180 days, is around 3.4 m/sec. The associated response is illustrated in Figure 1. Most of the total cost is incurred during the first six hours to correct the large injection error. The maximum thrust level required, for a 700 kg spacecraft, during this correction phase is around 0.85 N. However, once the nominal distance is achieved, the required thrust levels drop down to 10^{-9} N. In contrast, formations characterized by relative separation distances on the order of thousands of kilometers require nominal thrust levels on the order of 10^{-3} N.

Output Feedback Linearization (OFL)

Consider the relative equations of motion for the ith deputy as defined by Equation (1.5). Let $\bar{r}^{CD_i} = \bar{r}(t)$, $\Delta\bar{f}^{D_i} = \Delta\bar{f}\left(\bar{r}(t)\right)$, and $\bar{u}_{D_i}(t) = \bar{u}(t)$. Then, the relative equations of motion associated with the three-body problem

3

can be represented, in vector form, as $\ddot{\bar{r}}(t) = \Delta\bar{f}(\bar{r}(t)) + \bar{u}(t)$. The OFL controller, originally formulated in [1], seeks to identify the control input $\bar{u}(t)$ such that $\ddot{r} = g(\bar{r}, \dot{\bar{r}})$, where $g(\bar{r}, \dot{\bar{r}})$ is representative of the desired critically damped radial error response. Note that the OFL controller enforces only the radial distance constraint. The vehicle orientation is not explicitly controlled. This leads to a single scalar constraint that can be represented in the form

$$h(\bar{r}(t), \dot{\bar{r}}(t)) = \bar{u}(t)^T \bar{r}(t). \tag{1.9}$$

where $h(\bar{r}(t), \dot{\bar{r}}(t))$ is some nonlinear function of $\bar{r}(t)$ and $\dot{\bar{r}}(t)$. The expression in Equation (1.9) represents one equation in three unknowns, the three control accelerations in the input vector $\bar{u}(t)$. Since no additional constraint equations are imposed, there are an infinite number of solutions that satisfy Equation (1.9). In the initial investigation into the OFL controller [1], the left side of Equation (1.9) is factored in terms of $\bar{r}(t)$ to allow for an explicit solution for $\bar{u}(t)$. Although this particular solution satisfies the control goal, there are no guarantees or expectations of optimality. This particular formulation is based on the assumption that the measured output is defined as $y = r$. However, previously [15] and in the present study, formulations based on $y = r^2$ and $y = r^{-1}$ are also considered. Each of these measured output quantities leads to a different control law, as listed in Table 2. Furthermore, although the resulting control laws achieve the formation goal, as specified, the associated formation keeping costs can be <u>dramatically</u> different.

Table 2 – Summary of Control Laws and Formation Keeping Costs (Over 180 days)

as Determined in the Inertial Frame Associated with the Ephemeris Model

Output Vector	Control Law	Cumulative ΔV Over 180 Days
$y = r$	$\bar{u}(t) = \left\{ \dfrac{g(\bar{r}, \dot{\bar{r}})}{r} - \dfrac{\dot{\bar{r}}^T \dot{\bar{r}}}{r^2} \right\} \bar{r} + \left(\dfrac{\dot{r}}{r} \right) \dot{\bar{r}} - \bar{f}(\bar{r})$	2,342.2 m/sec
$y = r^2$	$\bar{u}(t) = \left\{ \dfrac{1}{2} \dfrac{g(\bar{r}, \dot{\bar{r}})}{r^2} - \dfrac{\dot{\bar{r}}^T \dot{\bar{r}}}{r^2} \right\} \bar{r} - \bar{f}(\bar{r})$	16,653.0 m/sec
$y = r^{-1}$	$\bar{u}(t) = \left\{ -rg(\bar{r}, \dot{\bar{r}}) - \dfrac{\dot{\bar{r}}^T \dot{\bar{r}}}{r^2} \right\} \bar{r} + 3 \left(\dfrac{\dot{r}}{r} \right) \dot{\bar{r}} - \bar{f}(\bar{r})$	50.8 m/sec

Since the control laws in Table 2 only enforce the radial distance constraint, and the relative orientation of the deputy with respect to the chief spacecraft is free, the nominal motion is equivalent to the deputy evolving on the surface of a sphere that is centered at the chief spacecraft. For some given initial state, $\bar{r}(0)$ and $\dot{\bar{r}}(0)$, the control laws listed in Table 2 essentially drive the deputy onto the surface of this nominal sphere. The corresponding trajectories converge onto the sphere following the prescribed critically damped dynamics. Numerical evidence suggests that the plane of motion of the deputy spacecraft is completely defined by the initial conditions, $\bar{r}(0)$ and $\dot{\bar{r}}(0)$. To better visualize this, consider the angular momentum quantity $\bar{h} = \bar{r} \times \dot{\bar{r}} = h\hat{h}$. As the control inputs described in Table 2 are applied, numerical analysis indicates that the direction of the angular momentum vector is fixed inertially (in the ephemeris model) while the magnitude follows a critically damped response onto some final converged value. If, instead, the formulation were associated with the synodic rotating frame [1, 15], the results indicate that the angular momentum direction is fixed in the rotating frame. The sample formation presented in Figure 2 is determined in the ephemeris model. The path of each of these vehicles is presented in the inertial frame. Hence, the converged relative orbits in Figure 2 are inertially fixed. It is also worth noting that the converged "orbital period" along the nominal sphere depends on the initial relative velocity of the vehicle, as illustrated in Figure 3.

To demonstrate the impact of the relative velocity of the deputy on the formation keeping cost, consider a nominal spherical formation characterized by a 5-km radial distance. Let $\bar{r}(0)$ and $\dot{\bar{r}}(0)$ denote the initial relative position and velocity vectors, respectively. For $\bar{r}(0) = 12\hat{x} - 5\hat{y} + 3\hat{z}$ km and $\dot{\bar{r}}(0) = \bar{0}$ m/sec the net formation keeping cost required to drive the deputy onto the surface of the nominal sphere is miniscule. However, as the relative velocity of the deputy increases, the OFL controller yields significantly higher costs. That is because the controller is trying to maintain a rotation rate specified by the initial velocity injection error, which is not consistent with the natural dynamics in the vicinity of the reference orbit. For the three output vectors defined in this study, the associated control inputs are summarized in Table 2. Also listed in Table 2 are the correction costs that correspond to an initial relative state defined by $\bar{r}(0) = 12\hat{x} - 5\hat{y} + 3\hat{z}$ km and $\dot{\bar{r}}(0) = \hat{x} - \hat{y} + \hat{z}$ m/sec. The associated nominal formation in this case is defined by a constant relative separation of 5 km.

CONTINUOUS VERSUS DISCRETE CONTROL

Based on results from previous investigations, [1, 3-5] it appears that it is possible, at least computationally, to achieve precise formations near the libration points if continuous control is both available and feasible. Howell and Marchand [1,15] demonstrate that continuous control methods, such as LQR and feedback linearization techniques, can mathematically enforce non-natural configurations but lead to extremely small control acceleration levels. For instance, for a 700 kg spacecraft, thrust levels can range between 10^{-3} N for a 5000 km formation to 10^{-9} N for a 50 meter formation. The thrust levels that are required, near the libration points, to maintain a small formation like TPF presently represent a technical challenge. Furthermore, although continuous control approaches are mathematically sound, the science goals of deep space missions may impose a series of constraints that eliminate continuous control as a feasible option. Some also suggest that maintaining a precise formation is, perhaps, ultimately not as critical as generating precise knowledge of the relative position of each spacecraft in the formation. In these cases, a discrete formation keeping strategy may represent an important capability.

DISCRETE CONTROL IN THE EPHEMERIS MODEL

Driven by control and/or implementation requirements, some new consideration is warranted concerning the degree of accuracy to which the formation can be maintained via discrete impulses. An LQR controller, based on a discrete time system, yields the optimal magnitude of each differential control impulse at specified time intervals. However, the value of the nominal control input that must be added is still assumed to be continuously available. So, in a truly discrete control strategy, how often must an impulsive maneuver be incorporated to maintain the desired configuration to some acceptable degree of accuracy, even in the presence of external perturbations?

Targeting A Nominal Relative State

Continuous control methods ensure that the desired nominal is enforced at each instant of time. However, if the formation keeping is discretized, how far will the vehicle configuration diverge from the specified nominal between maneuvers? Howell and Marchand [15] implement a simple targeter scheme that forces the vehicles in the formation to meet their nominal constraints at specified times during the mission. The impulsive scheme presented in [15] accomplishes the objective to within reasonable tolerances, provided the maneuvers are closely spaced. For instance, if $\bar{\rho}(t) = (10 \text{ m})\hat{Y}$ and a maneuver is performed once daily, the relative position of the deputy is always within 1 centimeter of the specified nominal, $\bar{\rho}(t)$. However, for a fixed maneuver interval, larger nominal separations lead to larger deviations from the nominal configuration in-between maneuvers. This deviation becomes significant for nominal separations on the order of kilometers. This suggests that nearly continuous control is required to precisely enforce large relative separations between the vehicles in the formation.

In general, achieving the desired nominal configuration to within extreme accuracy requires maneuvers that are fairly close to each other. However, this requirement introduces yet another difficulty. As the maneuvers become more closely spaced they also decrease in size. For a 10 meter nominal separation these maneuvers are on the order of 10^{-6} m/sec.

So, regardless of whether continuous or discrete control is available, accurately maintaining a <u>non-natural</u> nominal configuration, with small relative separations, is apparently not achievable with the technology presently available. Since the natural flow in this region of space is constantly acting against these non-natural configurations, the relative error increases rapidly if these small maneuvers are not accurately implemented. Conversely, formations that take advantage of the natural flow near the reference orbit require minimal station keeping beyond the initial injection maneuver.

Natural Formations

Understanding the natural flow near the libration points can be an extremely useful tool in constructing nominal formations and designing feasible control strategies that adequately enforce the desired configurations. Howell and Barden [8] previously identified naturally existing multi-spacecraft formations associated with a quasi-periodic torus that envelops a reference halo orbit in the CR3BP such as that illustrated in Figure 4(a). Their findings also reveal that these formations are preserved in the ephemeris model. Since this represents an unforced solution to the equations of motion, no control inputs are necessary. Howell and Marchand [15] identify another type of naturally existing formation analogous to a string of pearls, as illustrated in Figure 4(b). The surface illustrated in Figure 4(b) is traced by a quasi-periodic Lissajous trajectory near the Sun-Earth/Moon L_2 point, as determined in the SRP perturbed n-body ephemeris model. By properly phasing each vehicle, it is possible for the formation to naturally evolve along this surface such that the relative positions of each spacecraft in the formation are unaltered and the relative distances are closely bounded. That is, if the formation originates as a string of pearls, the orientation of the string is relatively unaffected in time, the lead vehicle always remains in the lead and the order of each subsequent vehicle along the "string of pearls" remains unchanged. Since each spacecraft in this formation evolves along a naturally existing Lissajous trajectory, maintaining this type of formation can be achieved with a standard station keeping approach.

During the development of a Floquet based controller, Howell and Marchand [15] also identify other types of naturally existing formations that utilize the flow along the stable and center manifold near the reference halo orbit. The controller is used to numerically identify these naturally existing formations as well as possible deployment into these configurations. The reference halo orbits of interest here are unstable. In particular, the eigenstructure of the associated linear system leads to one unstable mode, one stable mode, and four center modes. The unstable and stable modes are tangent to the local stable and unstable manifolds near the halo orbit, respectively. The center modes indicate the existence of bounded solutions near the reference orbit. For instance, two of these center modes lead to nearby periodic halo orbits. The other two modes, then, are associated with the torus in Figure 4(a). Given some initial state, the goal of the Floquet controller is to implement an impulsive maneuver that removes the unstable component of the relative state as well as the components associated with two of the four center modes. For a general set of initial conditions, this controller forces the deputy to follow a stable manifold path that converges onto a bounded solution near the reference halo orbit. This solution can be nearly periodic or quasi-periodic.

If the initial conditions are properly selected, $\bar{r}(0) = r_0 \hat{y}$, removing the unstable mode along with the two center modes associated with the torus, leads to the identification of nearly periodic relative orbits such as those illustrated in Figure 5. The eight spacecraft formation illustrated in Figure 5 is propagated over 1800 days. Though these orbits are actually expanding, the rate of expansion is very slow. In fact, propagation of these trajectories over a period of 18,000 days leads to solutions that area essentially identical to those in Figure 5. Nearly vertical orbits, associated with $\bar{r}(0) = r_0 \hat{z}$, also exist near the reference halo orbit, as illustrated in Figure 6. These are visibly expanding but at a very slow rate over the 1800 days of the integration. For initial conditions of the form $\bar{r}(0) = y_0 \hat{y} + z_0 \hat{z}$ the rate of expansion increases as $y_0 \to 0$ and $z_0 \to r_0$. This evolution is better visualized from Figure 7.

CONCLUSIONS

Mathematically, input and output feedback linearization techniques are effective in enforcing non-natural formations near the libration points, as determined in the SRP perturbed n-body ephemeris model. Input feedback linearization is effective in maintaining formations that are fixed in position and velocity relative to the reference "halo" orbit. Furthermore, in this region of space, the resulting error response and control input histories are

essentially identical to those obtained via LQR methods. IFL control, however, is not only conceptually simpler than time varying LQR methods, but it is also better suited for numerical implementation in the ephemeris model.

The present study also demonstrates that output feedback linearization techniques are effective in achieving inertially fixed circular orbits relative to a reference "halo" orbit. This is potentially useful for formations that seek spherical configurations evolving at non-natural rotation rates. The OFL control laws presented here are not fuel optimal, but the resulting thrust levels are physically achievable. Although fuel optimal is usually the goal for most missions, fuel optimal strategies for formations evolving near the libration points lead to extremely small thrust levels that are ultimately unrealistic given the present state of technology.

Nearly continuous control is essential if precise enforcement of these non-natural configurations is required to achieve the mission goals. However, precise formation keeping may not be necessary, given a possible shift to improved navigation and relative position information. Near the libration points, if maintaining a tight non-natural formation, via discrete impulses, is desired, frequent maneuvers are necessary. In this case, smaller maneuver intervals lead to smaller maneuvers. These can be on the order of 10^{-6} m/sec which raises an implementation issue.

The difficulties encountered with non-natural configurations may be overcome by developing a better understanding of the naturally existing formations. Although a nominal configuration <u>completely</u> consistent with the natural flow near the reference orbit is unlikely, understanding these naturally existing behaviors can lead to the development of techniques to construct formations that meet the mission objectives while exploiting the natural structure of the phase space. To that end, a series of naturally existing formations are also presented here.

REFERENCES

1. K.C. Howell and B.G. Marchand, "Control Strategies for Formation Flight in the Vicinity of the Libration Points," *AIAA/AAS Space Flight Mechanics Conference*, Ponce, Puerto Rico, Feb. 9-13, 2003. AAS Paper 03-113.

2. D.J. Scheeres and N.X. Vinh, "Dynamics and control of relative motion in an unstable orbit," *AIAA/AAS Astrodynamics Specialist Conference*, Denver, Colorado, Aug. 14-17, 2000. AIAA Paper 2000-4135.

3. P. Gurfil and N. J. Kasdin, "Dynamics and Control of Spacecraft Formation Flying in Three-Body Trajectories," *AIAA Guidance, Navigation, and Control Conference and Exhibit*, Montreal, Canada, Aug. 6-9, 2001. AIAA Paper 2001-4026.

4. P. Gurfil, M. Idan, and N. J. Kasdin, "Adaptive Neural Control of Deep-Space Formation Flying," *American Control Conference (ACC)*, Proceedings. Vol. 4, Anchorage, Alaska, May 8-10, 2002, p. 2842-2847.

5. R. J. Luquette and R. M. Sanner, "A Non-Linear Approach to Spacecraft Formation Control in the Vicinity of a Collinear Libration Point." *AAS/AIAA Astrodynamics Conference*; Proceedings, Quebec, July 30-Aug. 2, 2001, San Diego, California, p. 437-445.

6. N.H. Hamilton, "Formation Flying Satellite Control Around the L2 Sun-Earth Libration Point," M.S. Thesis, George Washington University, Washington, DC, December 2001.

7. D. Folta, J.R. Carpenter, and C. Wagner, "Formation Flying with Decentralized Control in Libration Point Orbits," International Symposium: Spaceflight Dynamics, Biarritz, France, June, 2000.

8. B.T. Barden and K.C. Howell, "Fundamental Motions Near Collinear Libration Points and Their Transitions," *The Journal of the Astronautical Sciences*, Vol. 46, No. 4, 1998, pp. 361-378.

9. B.T. Barden and K.C. Howell, "Formation Flying in the Vicinity of Libration Point Orbits," *Advances in Astronautical Sciences*, Vol. 99, Pt. 2, 1998, pp. 969-988.

10. B.T. Barden and K.C. Howell, "Dynamical Issues Associated with Relative Configurations of Multiple Spacecraft Near the Sun-Earth/Moon L1 Point," *AAS/AIAA Astrodynamics Specialists Conference*, Girdwood, Alaska, August 16-19, 1999, Paper No. AAS99-450.

11. K.C. Howell and B.T. Barden, "Trajectory Design and Stationkeeping for Multiple Spacecraft in Formation Near the Sun-Earth L1 Point," *IAF 50th International Astronautical Congress*, Amsterdam, Netherlands, Oct. 4-8, 1999. IAF/IAA Paper 99-A707.

12. G. Gómez, M. Lo, J. Masdemont, and K. Museth, "Simulation of Formation Flight Near Lagrange Points for the TPF Mission," AAS/AIAA Astrodynamics Conference, Quebec, Canada, July 30-Aug. 2, 2001. AAS 01-305.

13. K.C. Howell and T. Keeter, "Station-Keeping Strategies for Libration Point Orbits - Target Point and Floquet Mode Approaches," *Advances in the Astronautical Sciences,* Vol. 89, pt. 2, 1995, pp. 1377-1396.

14. G. Gómez, K.C. Howell, J. Masdemont, and C. Simó, "Station-keeping Strategies for Translunar Libration Point Orbits," *Advances in Astronautical Sciences*, Vol. 99, Pt. 2, 1998, pp. 949-967

15. B.G. Marchand and K.C. Howell, "Formation Flight Near L1 and L2 in the Sun-Earth/Moon Ephemeris System Including Solar Radiation Pressure," AAS/AIAA Astrodynamics Specialists Conference, Big Sky, Montana, August 3-7, 2003, Paper No. AAS03-596.

16. C.R. McInnes, *Solar Sailing: Technology, Dynamics and Mission Applications*, United Kingdom: Praxis Publishing Ltd, 1999.
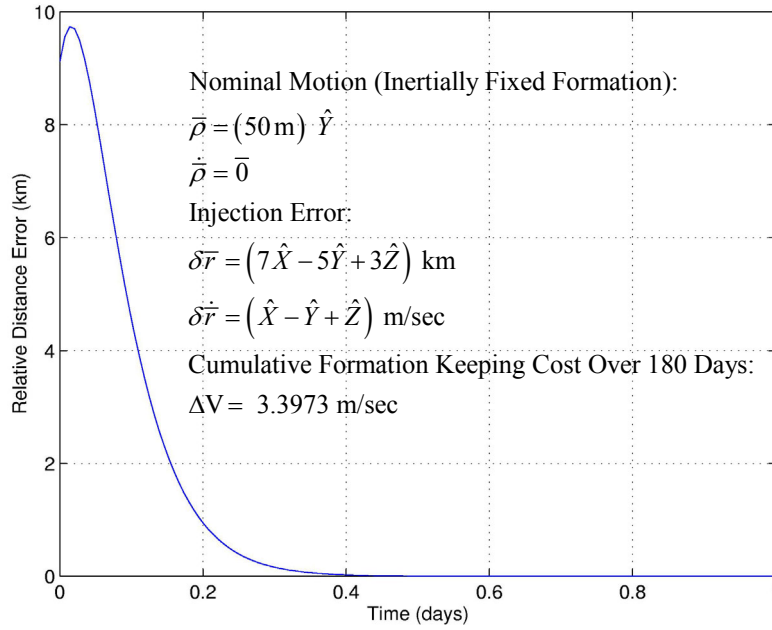
Nominal Motion (Inertially Fixed Formation):

$$\bar{\rho} = (50\,\text{m})\,\hat{Y}$$

$$\dot{\bar{\rho}} = \bar{0}$$

Injection Error:

$$\delta\bar{r} = \left(7\hat{X} - 5\hat{Y} + 3\hat{Z}\right)\,\text{km}$$

$$\delta\dot{\bar{r}} = \left(\hat{X} - \hat{Y} + \hat{Z}\right)\,\text{m/sec}$$

Cumulative Formation Keeping Cost Over 180 Days:

$$\Delta V = 3.3973\ \text{m/sec}$$

Figure 1 – IFL Response to Injection Error
as Determined in the Ephemeris Model of the Sun-Earth/Moon System

Inertial Frame
Perspective
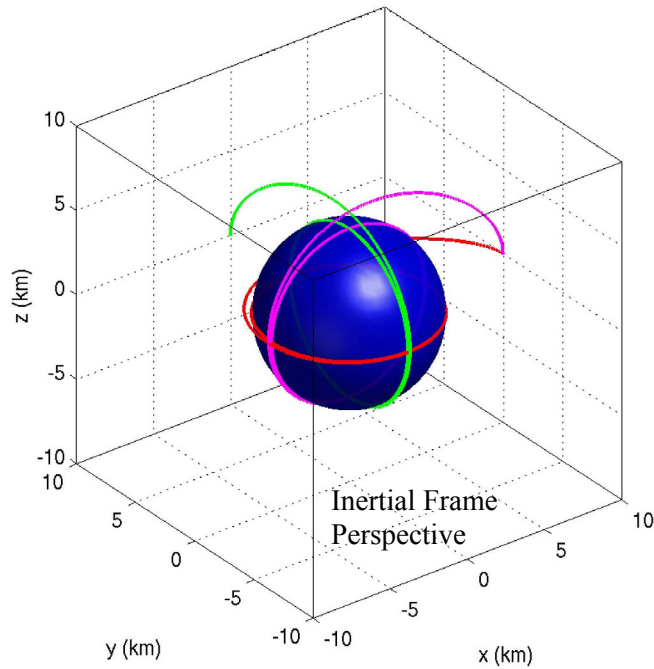
FIGURE 2 – OFL Controlled Response of Deputy Spacecraft Over 180 Days
as Determined in the Ephemeris Model of the Sun-Earth/Moon System
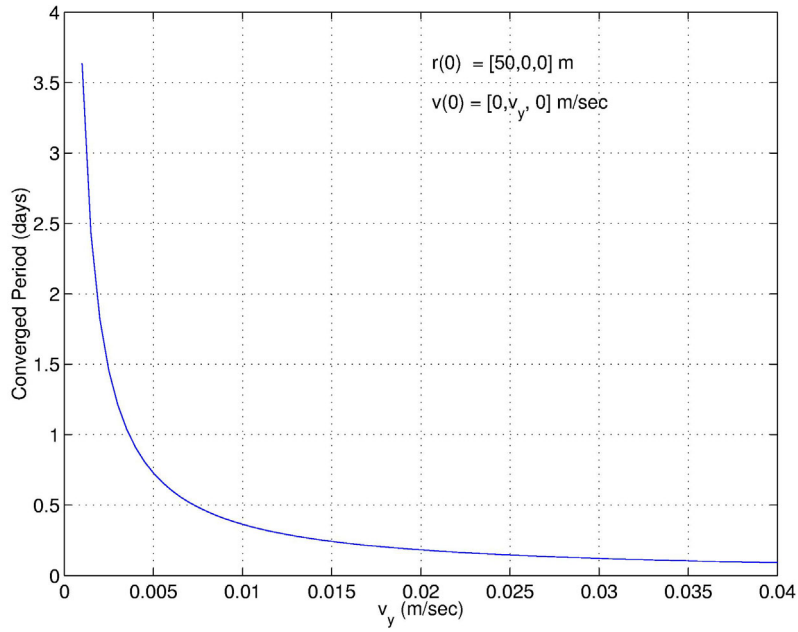
FIGURE 3 – Variation in Converged Period with Initial Relative Speed of Vehicle
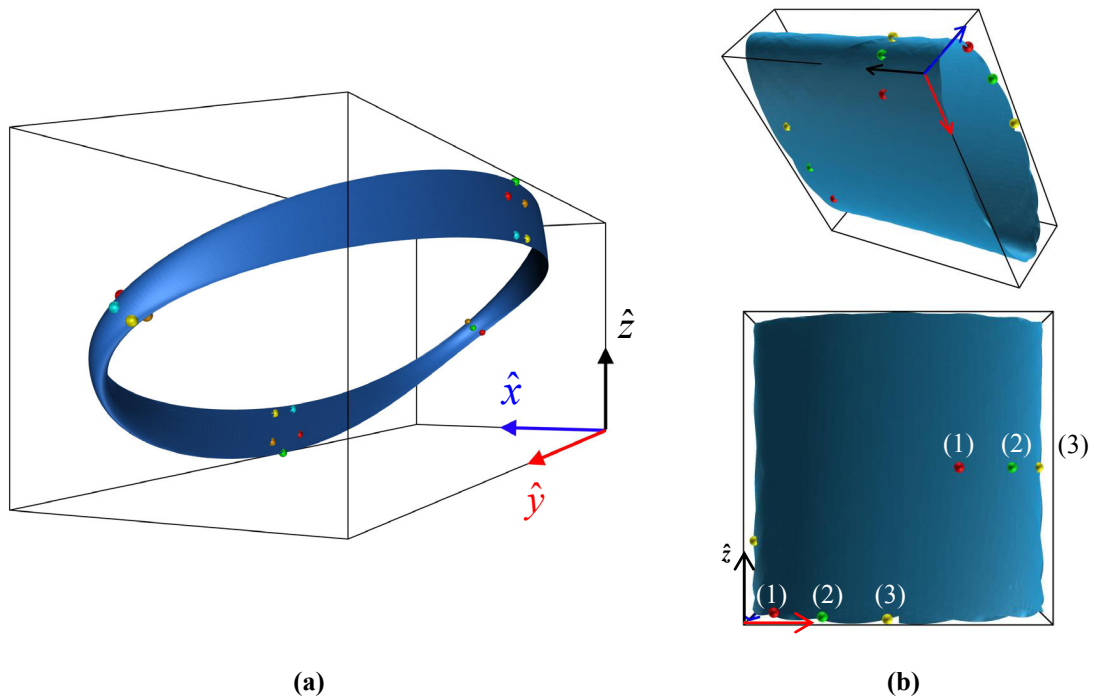for Spherical Formations Determined in the Ephemeris Model (OFL Control)

(a)

(b)

Figure 4 – Natural Torus (a) and "String of Pearls" (b) Formation in the Ephemeris Model
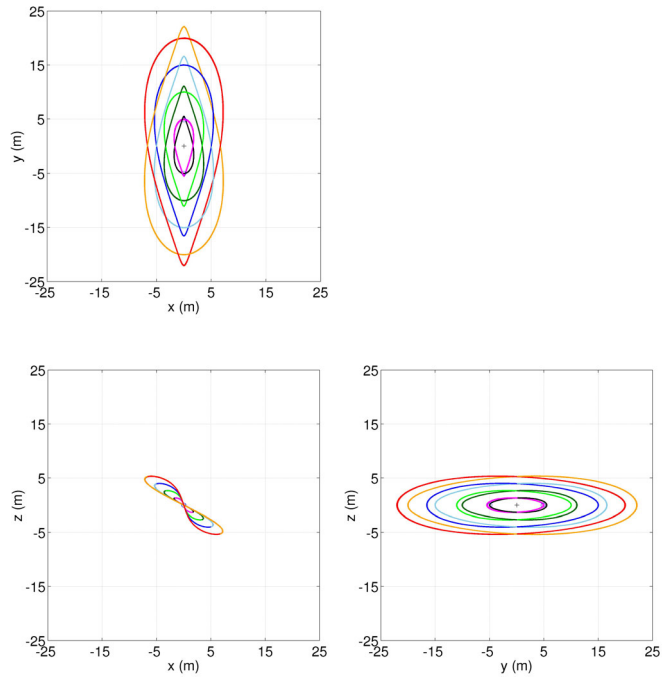
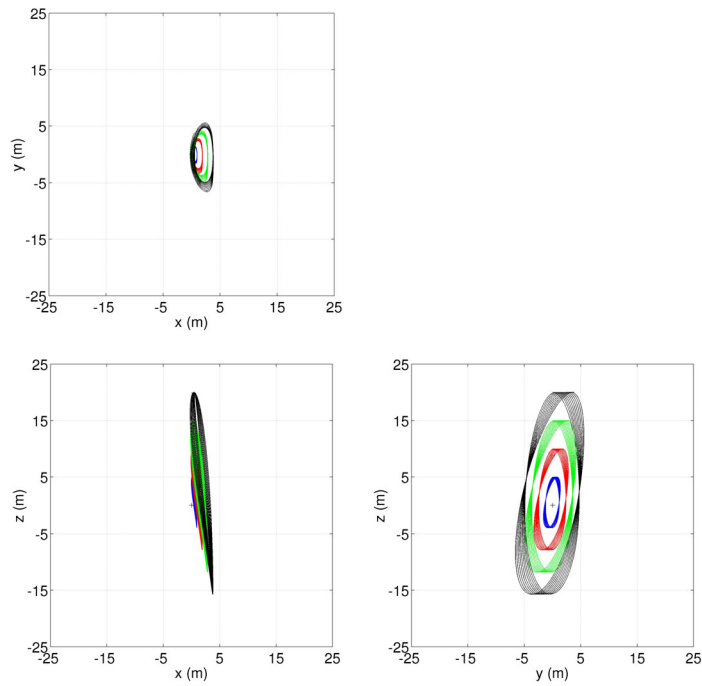**Figure 5 – Natural Eight Spacecraft Formation About a Single Chief S/C**

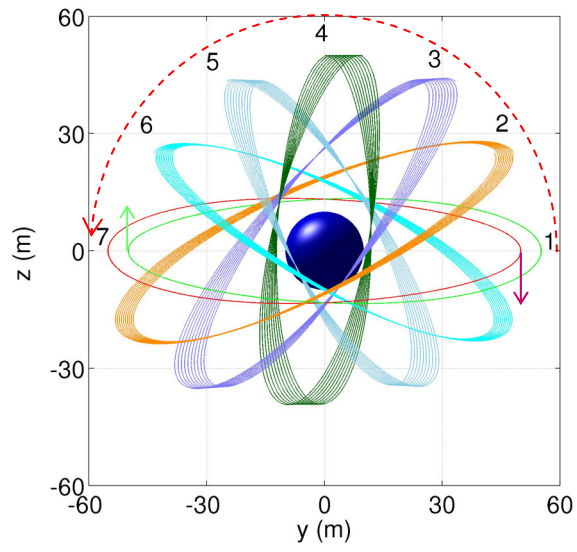**Figure 6 – Nearly Vertical Relative Orbits (4 S/C Formation)**

Figure 7 – Variation in Relative Orbit Expansion Rate Along the *yz*-plane